Systematic extraction of spectroscopic factors from $^{12}C(d,p)^{13}C$ and $^{13}C(p,d)^{12}C$ reactions

X. D. Liu, M. A. Famiano, W. G. Lynch, and M. B. Tsang
National Superconducting Cyclotron Laboratory and Department of Physics and Astronomy, Michigan State University, East Lansing, Michigan 48824, USA

J. A. Tostevin
Department of Physics, School of Electronics and Physical Sciences, University of Surrey, Guildford, Surrey GU2 7XH, United Kingdom

(Received 21 April 2004; published 14 June 2004)

Existing measurements of the angular distributions of the ground-state to ground-state transitions of the $^{12}C(d,p)^{13}C$ and $^{13}C(p,d)^{12}C$ neutron-transfer reactions have been analyzed systematically using the Johnson-Soper adiabatic and distorted-wave theories. When using a consistent set of physical inputs the deduced spectroscopic factors are consistent to within 15% for incident deuteron energies from 12 to 60 MeV. By contrast, original analyses of many of these data quoted spectroscopic factors that differed by up to a factor of 5. The present analysis provides an important reference point from which to assess the requirements of future spectroscopic analyses of transfer reactions measured in inverse kinematics using rare nuclei.

DOI: 10.1103/PhysRevC.69.064313 PACS number(s): 21.10.Jx, 24.50.+g, 27.20.+n

The ordering and occupancies of the single nucleon orbits influences the energies and angular momenta of low-lying quantum states of nuclei [1,2], as well as their decays and production rates in nuclear experiments and stellar environments [3]. Single-nucleon transfer reactions, such as $d+A \Rightarrow p+B$ and $p+B \Rightarrow d+A$, probe the wave functions of the transferred nucleon [1–6]. The overlap integral between the wave function of one state in nucleus A and another in B defines the theoretical spectroscopic factor for transfer between these states [5,6]. The ratio of the corresponding measured cross section divided by the cross section calculated for unit spectroscopic factor provides its experimental counterpart.

Spectroscopic information about the valence orbitals for unstable nuclei far from the valley of beta stability may lead to novel and surprising properties for the corresponding unstable nuclear states [7,8]. Single-nucleon transfer and knockout experiments in inverse kinematics with rare nuclei as projectiles, provide the optimal way to study neutron- and proton-rich nuclei and their single-particle states [3,9–12]. However, it is critical to understand the limitations of transfer reaction theories used to extract spectroscopic factors and to develop strategies to overcome them. Because data with rare isotope beams are limited, re-examining abundant and precise measurements made with light-ion beams such as ^{12}C and ^{13}C, may better test the consistency of such analyses.

Table I lists the past measurements of $^{12}C(d,p)^{13}C$(g.s.) reaction at incident energy above 4 MeV and its inverse reaction, $^{13}C(p,d)^{12}C$(g.s.) [13–38]. Figure 1 shows the published spectroscopic factors (SF) of the $p_{1/2}$ neutron coupled to the ^{12}C as a function of the equivalent incident deuteron energy up to 70 MeV. The extracted values from $^{12}C(d,p)^{13}C$(g.s.) (closed points) and $^{13}C(p,d)^{12}C$(g.s.) (open points) reactions fluctuate from 0.3 to 1.4 with no evident correlation with incident energy. In some analysis, multiple values were deduced from different optical model parameter sets or different theories; the higher values are shown for those cases as squares in Fig. 1. The dashed line marks the theoretical prediction (0.62) of the Cohen and Kurath shell model calculation [39].

Large uncertainties have been associated with the extraction of spectroscopic factors from the (p,d) and (d,p) transfer reactions [40]. Using consistency checks between inverse reactions involving *sd*-shell nuclei, for example, Endt [40] extracted an error of about 50% for individual spectroscopic factors from (p,d) and (d,p) reactions. Such large uncertainties make it difficult to extract consistently meaningful empirical spectroscopic factors that can be compared to theoretical values.

The sensitivity of calculations to the optical model potentials assumed in the entrance and exit channels constitutes the most significant problem in the extraction of spectroscopic factors from DWBA analyses of transfer reactions [5]. The deduced spectroscopic factors are dependent on these choices; thus, many have measured elastic scattering data at the entrance and exit energies to fix the optical model parameters. Such data may be difficult to obtain at the desired energy. Moreover, their use may introduce spurious energy dependences stemming from detailed coupled-channel or compound resonance effects. Our analyses minimize the need for such data and show that superior results can be achieved by the consistent use of reasonable global optical potentials.

In the following, we use phenomenological global nucleon optical potentials [41–46] and potentials based on microscopic methods, such as the Jeukenne-Lejeune-Mahaux (JLM) effective nucleon-nucleon interaction [47,48]. To assess the systematic uncertainties associated with the extraction of spectroscopic factors, we analyze the angular distributions of the differential cross section of the $^{12}C(d,p)^{13}C$(g.s.) reaction and of its inverse, $^{13}C(p,d)^{12}C$(g.s.). Using reasonable theoretical inputs, we extract a consistent value (to within 15%) for the spectroscopic factor of the $p_{1/2}$ neutron coupled to the ^{12}C(g.s.) over

TABLE I. Past measurement of $^{12}C(d,p)^{13}C_{g.s.}$ and $^{13}C(p,d)^{12}C_{g.s.}$ reactions.

E_{beam}(MeV)	SF (published)	SF (JLM)	SF (CH)	SF (DWBA)	Ref.
$^{12}C(d,p)^{13}C_{g.s.}$					
4	0.99	0.62	0.61	0.65	[14]
4.5	0.72	0.69	0.69	0.6	[14]
4.5		0.52	0.53	0.4	[15]
4.5	0.55,0.6,0.8	0.42	0.43	0.49	[16]
7.15	0.53	0.89	0.93	0.94	[17]
8.9		0.8	0.9	0.91	[18]
9.0	0.84	N/A	N/A	N/A	[19]
10.2		0.68	0.79	0.81	[20]
11.8		0.61	0.74	0.77	[21]
12	1.15	0.50	0.63	0.68	[22]
12	1.16,0.64,0.83,0.85	0.75	0.85	0.86	[23–25]
12.4		0.63	0.74	0.78	[20]
14.7		0.61	0.74	0.79	[20]
14.8		0.64	0.75	0.78	[26]
15	1.1,1.4	0.53	0.67	0.74	[27]
16.6	0.85	0.48	0.59	0.66	[28]
19.6		0.52	0.65	0.76	[28]
25.9	0.7	0.59	0.69	0.79	[29]
28		N/A	N/A	N/A	[30]
30	0.77	0.52	0.65	0.79	[31]
51	0.95	0.66	0.82	1.06	[32,33]
56	0.63,0.75,1.26	N/A	N/A	N/A	[34]
$^{13}C(p,d)^{12}C_{g.s.}$					
35	0.7,0.8,1.0	0.66	0.85	1.16	[35]
41.3	0.91,0.98	0.78	0.98	1.31	[36]
55	0.82	0.66	0.82	1.05	[37]
65	0.26,0.31,0.43	N/A	N/A	N/A	[38]

a wide range of incident energies from 12 to 60 MeV. The remaining variations in the spectroscopic factor may partly stem from uncertainties in the measured differential cross sections.

First, we focus on the $^{12}C(d,p)$ angular distributions, shown in Fig. 2, that have been measured at incident energies ranging from 7 MeV to 56 MeV. Each distribution is offset by factors of 10 from the neighboring distributions for ease of presentation, the overall normalization factor being unity for the 19.6 MeV angular distribution. The spectroscopic factor is extracted by fitting the theory to the data at the first peak in the angular distribution, since the backward angle data are more sensitive to the effects of inelastic couplings and other higher-order effects. To be consistent, the spectroscopic factors are extracted by minimizing χ^2, including only angular points that are (i) within 30% of the predicted maximum yield and (ii) at $\theta_{c.m.} < 30°$. A similar analysis is also performed on data from the inverse reaction of $^{13}C(p,d)^{12}C$(g.s.) for proton incident energies ranging from 35 to 65 MeV [35–38].

Our calculations analyze all data sets in a consistent way and use a modified version of the code TWOFNR [49]. All calculations make the local energy approximation (LEA) for finite range effects [50] using the zero-range strength (D_0) and range (β) parameters of the Reid soft-core $^3S_1-^3D_1$ neutron-proton interaction [51]. The $1p_{1/2}$ neutron binding potential had radius parameter 1.25 fm and diffuseness 0.65 fm; variations of 5% in the radius and diffuseness caused 5% and 3% variations in the extracted spectroscopic factors, respectively. The depth of the potential is normalized to the experimental binding energy. For simplicity, no spin-orbit coupling is included in the calculations. Inclusion of the spin-orbit potential increases the spectroscopic factors by about 6–8 %. Nonlocality corrections [52] with range parameters of 0.85 and 0.54 are included in the proton and deuteron channels, respectively.

We calculate the transfer cross sections within the Johnson-Soper (JS) adiabatic approximation to the neutron, proton, and target three-body system [53], which includes the effects of break up of the deuteron in the field of the target, and requires *only* a specification of the nucleon-target interactions. The exact (d,p) and (p,d) transfer reaction amplitudes require knowledge of the adiabatic three-body wave function only at small neutron-proton separations. There, the adiabatic distorting potential governing the center-of-mass motion of the deuteron is well described by the sum of the

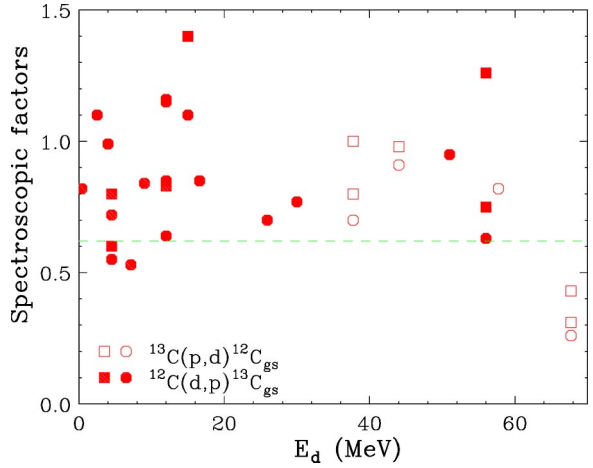

FIG. 1. (Color online) Spectroscopic factors for $^{12}C(d,p)^{13}C$(g.s.) and $^{13}C(p,d)^{12}C$(g.s.) reactions extracted from the literature (see Table I).

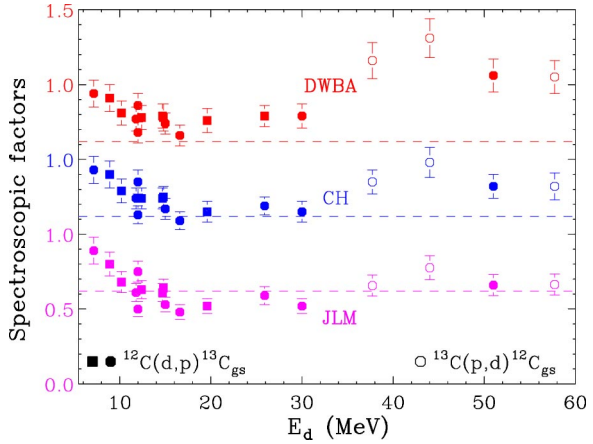

FIG. 3. (Color online) Extracted spectroscopic factors in the present work for $^{12}C(d,p)^{13}C$ and $^{13}C(p,d)^{12}C$ reactions. The dashed lines represent the shell model prediction of Cohen and Kurath [39] of 0.62. Results from three different calculations using the parameters summarized in Table II are shown. See text for detail explanation.

neutron- and proton-target optical potentials [53]. It is important to stress that this adiabatic distorting potential generates the three-body wave function in that limited region of configuration space needed to evaluate the transfer amplitude. It does not describe deuteron elastic scattering at the beam energy.

We first perform (d,p) calculations where both the exit channel proton potential and the entrance channel JS adiabatic potential use the JLM nucleon-target optical potentials [54]. These are calculated by folding the density-dependent JLM nucleon-nucleon effective interaction [47,48], assumed to have a Gaussian form factor of range 1 fm [55], with the assumed target matter density in the midpoint local-density approximation [55]. The matter density distributions for both ^{12}C and ^{13}C are evaluated assuming the modified oscillator density parameters ($\alpha=1.247$, $a=1.649$ fm for ^{12}C; $\alpha=1.403$, $a=1.635$ fm for ^{13}C) compiled in Ref. [56]. The corresponding root-mean-square (rms) charge radii are

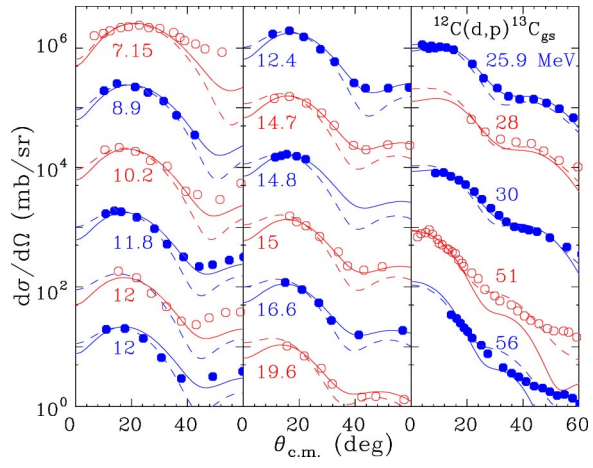

FIG. 2. (Color online) Angular distributions for $^{12}C(d,p)^{13}C$ reactions for beam energy from 7 to 56 MeV. Each distribution is displaced by factors of 10 from adjacent distributions. The overall normalization factor is 1 for the 19.6 MeV data. References are listed in Table I.

2.46 fm and 2.44 fm for ^{12}C and ^{13}C, respectively. The real and imaginary parts of the calculated nucleon optical potentials were scaled by multiplicative factors $\lambda_v=1.0$ and $\lambda_w=0.8$, obtained from a systematic study of light nuclei [54].

The calculated angular distributions normalized by the extracted spectroscopic factors are shown as solid lines in Fig. 2. The associated spectroscopic factors, shown at the bottom of Fig. 3, include reanalyses of the data in Fig. 1 (closed circles) [17,22,23,27–29,31,33] and of additional data sets (closed squares) [18,20,21,26,28]. Above 35 MeV, we supplement the limited (d,p) data with $^{13}C(p,d)$ data [35–38] denoted by the open symbols in Figs. 1 and 3. We did not analyze data at $E_d=28$ [30] and 56 MeV [34], and at $E_p=65$ MeV [38] because those angular distributions did not include the first peak.

The rise of the spectroscopic factors with decreasing energy below 12 MeV shown in Fig. 3 has been observed before [23] and has been attributed to the effect of resonance structures in the elastic scattering of deuterons [57] and the $^{12}C(d,p)$ reactions [58]. Excluding measurements affected by compound nucleus formation and resonances, the spectroscopic factors deduced for $E_d=12-60$ MeV provide an average spectroscopic factor of 0.61 ± 0.09. In contrast, the published values in Fig. 1 vary from 0.3 to 1.5. Our consistent, theoretically motivated analyses reduce the fluctuations substantially. If we examine the spread of the measurements for overlapping sets of data at $E_d\sim4.5,12$, and 15 MeV, it is clear that the measured angular distributions do not agree to better than 20%. Thus the uncertainties of the spectroscopic factors mainly come from the experimental measurements.

To assess the stability of the above adiabatic three-body model calculations, we have repeated these analyses while replacing the JLM nucleon optical potentials everywhere by the Chapel-Hill (CH) [43] global potential set. The spectroscopic factors are shown in the center of Fig. 3. Overall, the values are quite similar, but are consistently somewhat higher. The average spectroscopic factor is 0.75 ± 0.10. It

TABLE II. Summary of the input parameters used in TWOFNR.

	DWBA	Adiabatic CH	JLM
Proton potential	Chapel-Hill [43]	Chapel-Hill [43]	JLM [47,48]
Deuteron potential	Daehnick [45]	Adiabatic [53] from CH	Adiabatic [53] from JLM
Target densities			Modified harmonic oscillator density [56]
			$\alpha=1.247, a=1.649$ fm ^{12}C
			$\alpha=1.403, a=1.635$ fm ^{13}C
n-binding potential	Woods-Saxon,	Woods-Saxon,	Woods-Saxon,
	$r_0=1.25, a=0.65$	$r_0=1.25, a=0.65$	$r_0=1.25, a=0.65$
Hulthen finite range factor [51]	0.7457	0.7457	0.7457
Vertex constant D_0^2 [51]	15 006.25	15 006.25	15 006.25
JLM potential scaling λ	N/A	N/A	$\lambda_v=1.0$ and $\lambda_w=0.8$ [54]
Nonlocality potentials	*p* 0.85; *n* N/A; *d* 0.54	*p* 0.85; *n* N/A; *d* 0.54	*p* 0.85; *n* N/A; *d* 0.54

should be noted that light nuclei were not included in the database for the CH potential evaluation. A consistent use of alternative global nucleon potentials, such as that of Becchetti and Greenlees [44] leads to very similar results.

For a final comparison, we also analyzed the full data set within the DWBA formalism, neglecting the role of deuteron break-up channels. To remove energy-dependent optical potential ambiguity, we used the CH and Daehnick [45] global potentials for the proton and deuteron channels, respectively. The calculated angular distributions normalized by the spectroscopic factors are shown by the dashed curves in Fig. 2 and the deduced spectroscopic factors are plotted at the top of Fig. 3. The average value is 0.87 ± 0.19. For the higher energies, the values are larger. Comparisons with the JS adiabatic calculations suggest that neglect of the break-up channel within the DWBA may be a significant contributing factor at these higher energies.

In summary, published analyses of angular distributions for the ^{12}C$(d,p)^{13}$C(g.s.) and ^{13}C$(p,d)^{12}$C(g.s.) reactions display considerable variations in the extracted spectroscopic factors. Using consistent optical potential parametrizations and fitting the first maximum in the angular distributions provide spectroscopic factors that are consistent to within 15% for $E_d=12-60$ MeV. This energy range spans the optimum angular and linear momentum matching conditions for (d,p) and (p,d) transfer reaction studies. The use of global optical potentials or the JLM potential parametrization results in consistent values for the spectroscopic factor at each energy; the absolute values depend somewhat on the choice of potentials used but the values are close to the theoretical values suggesting that the input parameters we use in the distorted wave theory calculations are reasonable.

The global parametrization of the optical model potentials requires the minimum input parameter choice and may be advantageous where it is not important to extract the absolute spectroscopic factors. These global parametrizations, however, are fitted only to data from stable nuclei. In neutron and proton-rich regions of the nuclear chart, the use of microscopic optical potentials like the JLM, but folded with Hartree-Fock matter densities for the relevant nuclei may offer a more realistic alternative. The current analysis of ^{12}C$(d,p)^{13}$C and ^{13}C$(p,d)^{12}$C reactions provide a reference point in the *p*-shell nuclei to which relative spectroscopic factors can be measured. The input parameters, summarized in Table II, should be applicable to other systems. Future studies of different systems are needed to guide the broadly based programs to investigate the single particle structure of rare isotopes with the operation of current and future intense rare isotope facilities.

This work was supported by the National Science Foundation under Grant No. PHY-01-10253 and by the U.K. Engineering and Physical Sciences Research Council through Grant No. GR/M82141.

[1] N. Austern, *Direct Nuclear Reaction Theories* (Wiley, New York, 1970).
[2] G. R. Satchler, *Direct Nuclear Reactions* (Oxford University Press, Oxford, 1983).
[3] W. N. Catford, Nucl. Phys. **A701**, 1c (2002).
[4] S. T. Butler, Proc. R. Soc. London, Ser. A **208**, 559 (1951).
[5] M. H. Macfarlane and J. B. French, Rev. Mod. Phys. **32**, 567 (1960).
[6] M. H. Macfarlane and J. P. Schiffer, *Nuclear Spectroscopy and Reactions* (Academic, New York, London, 1974), Vol. 40B, pp. 170–194.
[7] P. G. Hansen, A. S. Jensen, and B. Jonson, Annu. Rev. Nucl. Part. Sci. **45**, 591 (1995).
[8] V. Maddalena *et al.*, Phys. Rev. C **63**, 024613 (2001).
[9] P. G. Hansen and B. M. Sherrill, Nucl. Phys. **A693**, 133 (2001).
[10] P. G. Hansen and J. A. Tostevin, Annu. Rev. Nucl. Part. Sci. **53**, 219 (2003).
[11] S. Fortier *et al.*, Phys. Lett. B **461**, 22 (1999).
[12] J. S. Winfield *et al.*, Nucl. Phys. **A683**, 48 (2001).

[13] G. D. Putt, Nucl. Phys. **A161**, 547 (1971).
[14] A. Gallmann, P. Fintz, and P. E. Hodgson, Nucl. Phys. **82**, 161 (1966).
[15] T. W. Bonner, J. T. Eisinger, A. A. Kraus, Jr., and J. B. Marion, Phys. Rev. **101**, 209 (1956).
[16] H. Guratzsch, G. Hofmann, H. Müller, and G. Stiller, Nucl. Phys. **A129**, 405 (1969).
[17] N. I. Zaika, O. F. Nemets, and S. Tserino, Sov. Phys. JETP **12**, 1 (1961).
[18] D. Robson, Nucl. Phys. **22**, 34 (1961).
[19] W. R. Smith and E. V. Ivash, Phys. Rev. **131**, 304 (1963).
[20] E. W. Hamburger, Phys. Rev. **123**, 619 (1961).
[21] U. Schmidt-Rohr, R. Stock, and P. Turek, Nucl. Phys. **53**, 77 (1964).
[22] J. Lang *et al.*, Nucl. Phys. **A477**, 77 (1988).
[23] J. P. Schiffer, G. C. Morrison, R. H. Siemssen, and B. Zeidman, Phys. Rev. **164**, 1274 (1967).
[24] J. Dobes, Nucl. Phys. **A157**, 661 (1970).
[25] K. A. Gridnev and E. F. Hefter, Z. Phys. A **273**, 99 (1975).
[26] J. N. McGruer, E. K. Warburton, and R. S. Bender, Phys. Rev. **100**, 235 (1955).
[27] S. E. Darden, S. Sen, H. R. Hiddleston, J. A. Aymar, and W. A. Yoh, Nucl. Phys. **A208**, 77 (1973).
[28] S. Morita, N. Kawai, N. Takano, Y. Goto, R. Hanada, Y. Nakajima, S. Takemoto, and Y. Taegashi, J. Phys. Soc. Jpn. **15**, 550 (1960).
[29] R. van Dantzig and L. A. CH. Koerts, Nucl. Phys. **48**, 177 (1963).
[30] R. J. Slobodrian, Phys. Rev. **126**, 1059 (1962).
[31] H. Ohnuma, N. Hoshino, O. Mikoshiba, K. Raywood, A. Sakaguchi, G. G. Shute, B. M. Spicer, M. H. Tanaka, M. Tanifuji, T. Terasawa, and M. Yasue, Nucl. Phys. **A448**, 205 (1986).
[32] L. J. B. Goldfarb and E. F. Hefter, Phys. Lett. **38B**, 379 (1972).
[33] W. Fetscher, K. Sattler, E. Seibt, R. Staudt, and Ch. Weddigen, in *Proceedings of the Third International Symposium on Polarization Phenomena in Nuclear Reactions*, edited by H. H. Barschall and W. Haeberli (University of Wisconsin Press, Madison, 1971), p. 772.
[34] K. Hatanaka, N. Matsuoka, T. Saito, K. Hosono, M. Kondo, S. Kato, T. Higo, S. Matsuki, Y. Kadota, and K. Ogino, Nucl. Phys. **A419**, 530 (1984).
[35] H. Toyokawa, H. Ohnuma, Y. Tajima, T. Niizeki, Y. Honjo, S. Tomita, K. Ohkushi, M. H. Tanaka, S. Kubono, and M. Yosoi, Phys. Rev. C **51**, 2592 (1995).
[36] J. R. Campbell, W. R. Falk, N. E. Davison, J. Knudson, R. Aryaeinejad, and R. Tkachuk, Nucl. Phys. **A470**, 349 (1987).
[37] H. Taketani, J. Muto, H. Yamaguchi, and J. Kokame, Phys. Lett. **27B**, 625 (1968).
[38] K. Hosono, M. Kondo, T. Saito, N. Matsuoka, S. Nagamachi, T. Noro, H. Shimizu, S. Kato, K. Okada, K. Ogino, and Y. Kadota, Nucl. Phys. **A343**, 234 (1980).
[39] S. Cohen and D. Kurath, Nucl. Phys. **A101**, 1 (1967).
[40] P. M. Endt, At. Data Nucl. Data Tables **19**, 23 (1977).
[41] C. M. Perey and F. G. Perey, At. Data Nucl. Data Tables **17**, 1 (1976).
[42] J. J. H. Menet, E. E. Gross, J. J. Malanify, and A. Zucker, Phys. Rev. C **4**, 1114 (1971).
[43] R. L. Varner, W. J. Thompson, T. L. McAbee, E. J. Ludwig, and T. B. Clegg, Phys. Rep. **201**, 57 (1991).
[44] F. D. Becchetti, Jr. and G. W. Greenlees, Phys. Rev. **182**, 1190 (1969).
[45] W. W. Daehnick, J. D. Childs, and Z. Vrcelj, Phys. Rev. C **21**, 2253 (1980).
[46] J. M. Lohr and W. Haeberli, Nucl. Phys. **A232**, 381 (1974).
[47] J.-P. Jeukenne, A. Lejeune, and C. Mahaux, Phys. Rev. C **15**, 10 (1977).
[48] J.-P. Jeukenne, A. Lejeune, and C. Mahaux, Phys. Rev. C **16**, 80 (1977).
[49] M. Igarashi *et al.*, computer program TWOFNR (Surrey University version).
[50] P. J. A. Buttle and L. J. B. Goldfarb, Proc. Phys. Soc. London **83**, 701 (1964).
[51] L. D. Knutson, J. A. Thomson, and H. O. Meyer, Nucl. Phys. **A241**, 36 (1975).
[52] F. Perey and B. Buck, Nucl. Phys. **32**, 353 (1962).
[53] R. C. Johnson and P. J. R. Soper, Phys. Rev. C **1**, 976 (1970).
[54] J. S. Petler, M. S. Islam, R. W. Finlay, and F. S. Dietrich, Phys. Rev. C **32**, 673 (1985).
[55] S. Mellema, R. W. Finlay, F. S. Dietrich, and F. Petrovich, Phys. Rev. C **28**, 2267 (1983).
[56] C. W. De Jager, H. De Vries, and C. De Vries, At. Data Nucl. Data Tables **14**, 479 (1974).
[57] G. G. Ohlsen and R. E. Shamu, Nucl. Phys. **45**, 523 (1963).
[58] J. E. Evans, J. A. Kuehner, and E. Almqvist, Phys. Rev. **131**, 1632 (1963).